HOKKAIDO UNIVERSITY

Title	Inhibition of Marburg Virus Budding by Nonneutralizing Antibodies to the Envelope Glycoprotein
Author(s)	Kajihara, Masahiro; Marzi, Andrea; Nakayama, Eri et al.
Citation	Journal of Virology, 86(24), 13467-13474 https://doi.org/10.1128/JVI.01896-12
Issue Date	2012-12
Doc URL	https://hdl.handle.net/2115/52795
Rights	© 2012 American Society for Microbiology
Type	journal article
File Information	JV86-24_13467-13474.pdf

Hokkaido University Collection of Scholarly and Academic Papers : HUSCAP

Inhibition of Marburg virus budding by nonneutralizing antibodies to the envelope glycoprotein

Masahiro Kajihara[1], Andrea Marzi[2], Eri Nakayama[1], Takeshi Noda[3], Makoto Kuroda[1], Rashid Manzoor[1], Keita Matsuno[1], Heinz Feldmann[2], Reiko Yoshida[1], Yoshihiro Kawaoka[3, 4, 5, 6], and Ayato Takada[1, 7]*

[1]Division of Global Epidemiology, Hokkaido University Research Center for Zoonosis Control, Sapporo 001-0020, Japan

[2]Laboratory of Virology, Division of Intramural Research, National Institute of Allergy and Infectious Diseases, National Institutes of Health, Rocky Mountain Laboratories, Hamilton, Montana, USA

[3]Division of Virology, Department of Microbiology and Immunology, Institute of Medical Science, University of Tokyo, Shirokanedai, Minato-ku, Tokyo 108-8639, Japan

[4]International Research Center for Infectious Diseases, Institute of Medical Science, University of Tokyo, Shirokanedai, Minato-ku, Tokyo 108-8639, Japan

[5]ERATO Infection-induced Host Responses Project, Saitama 332-0012, Japan

[6]Department of Pathobiological Science, University of Wisconsin-Madison, Madison, Wisconsin 53711, USA

[7]School of Veterinary Medicine, the University of Zambia, P. O. Box 32379, Lusaka, Zambia

Running title: Antibodies inhibiting Marburg virus budding

*Corresponding author: Ayato Takada; email: atakada@czc.hokudai.ac.jp

Word count: Abstract 208 words, Text 4,359 words.

Abstract

The envelope glycoprotein (GP) of Marburg virus (MARV) and Ebola virus (EBOV) is responsible for virus entry into host cells and known as the only target of neutralizing antibodies. While knowledge about EBOV neutralizing antibodies and the mechanism for neutralization of infectivity is being accumulated gradually, little is known about antibodies that can efficiently regulate MARV infectivity. Here we show that MARV GP-specific monoclonal antibodies AGP127-8 (IgG1) and MGP72-17 (IgM), which do not inhibit GP-mediated entry of MARV into host cells, drastically reduced budding and release of progeny viruses from infected cells. These antibodies similarly inhibited the formation of virus-like particles (VLPs) consisting of GP, the viral matrix protein, and nucleoprotein, whereas the Fab fragment of AGP127-8 showed no inhibitory effect. Morphological analyses revealed that filamentous VLPs were bunched on the surface of VLP-producing cells cultured in the presence of the antibodies. These results demonstrate a novel mechanism of antibody-mediated inhibition of MARV budding in which antibodies arrest unformed virus particles on the cell surface. Our data lead to the idea that such antibodies, like classical neutralizing antibodies, contribute to protective immunity against MARV and that the "classical" neutralizing activity is not the only indicator of a protective antibody that may be available for prophylactic and therapeutic use.

Introduction

Marburg virus (MARV) has a nonsegmented, single-stranded negative-sense RNA genome and, together with Ebola virus (EBOV), constitutes the family *Filoviridae* (30). Since the first cases of MARV infection were documented in Germany and Yugoslavia in 1967, sporadic outbreaks of Marburg hemorrhagic fever have been reported mainly from Central Africa (23). The case fatality rate of the largest outbreak in Angola in 2004-05 reached 88%. Although MARVs were isolated from Egyptian fruit bats (*Rousettus aegyptiacus*) in Uganda (42), the transmission routes to humans and nonhuman primates and the mechanisms whereby MARVs are perpetuated in nature are not fully understood. Currently, there is neither effective prophylaxis nor treatment available for filovirus infection. Thus, together with Ebola virus, MARV poses a significant public health threat in Central Africa, and is feared worldwide as a potentially imported infectious pathogen and a biothreat agent.

Filovirus particles consist of at least seven structural proteins, including the sole transmembrane glycoprotein (GP) on their surface. GP undergoes proteolytic cleavage by host proteases such as furin, resulting in the two subunits, GP1 and GP2, which are linked by a disulfide bond (46). GP is highly glycosylated with large amounts of N- and O-linked glycans, most of which are located in its middle one-third, designated the mucin-like region (5, 6). The primary function of GP is as a mediator of virus entry into host cells (40, 50), and therefore GP is believed to be the only target of neutralizing antibodies against filoviruses.

Previous studies focusing on the interaction between EBOV GP and neutralizing monoclonal antibodies (MAbs) indicate that direct inhibition of GP attachment to its ligand(s)/receptor(s) or fusion of viral and host cell membranes are likely to be key mechanisms of neutralization (17, 33, 38). Our most recent study demonstrated that passive immunization with well-characterized neutralizing MAbs had beneficial effects in a nonhuman primate model of Ebola hemorrhagic fever (21), highlighting the potential of antibody therapy against filovirus

infection. In contrast, little is known about MAbs efficiently neutralizing MARV infectivity *in vitro* and the mechanisms of antibody-mediated inhibition of MARV infectivity, although passive prophylaxis with polyclonal IgG antibodies was shown to protect nonhuman primates from lethal MARV infection (4).

While the virion structural protein (VP) 40, the major viral matrix protein, is the key driving force for budding of progeny virions (10, 11, 18, 27, 41), filovirus GPs are also known to be involved in the virus budding process. EBOV GP-expressing cells produce virosome-like structures possessing GP spikes on their surface, although these particles are pleomorphic and not similar morphologically to authentic virions (27). Furthermore, upon coexpression of GP and VP40 in cultured cells, virus-like particles (VLPs) morphologically resembling authentic virions are efficiently released into culture media (27, 43). This outward machinery (i.e., virus budding), indispensable for viral replication and dissemination, might be another target of protective antibodies. It is known that nonneutralizing antibodies against influenza A virus neuraminidase, which mediates the release of progeny viruses from host cells, play a role in protective immunity (12, 26, 48). It has also been demonstrated *in vitro* that the particle release of some viruses (e.g., bovine leukemia, vaccinia, sendai, and rubella viruses) from infected cells was reduced in the presence of MAbs or antiserum (1, 2, 28, 45).

In this study, we found that murine MAbs AGP127-8 and MGP72-17 remarkably reduced extracellular release of MARV from infected cells, whereas these antibodies did not inhibit GP-mediated entry of MARV into host cells. We further confirmed that AGP127-8 and MGP72-17 decreased the amount of VLPs produced by cells expressing GP, VP40, and nucleoprotein (NP) of MARV, suggesting that the MAbs inhibited budding of progeny virions from infected cells. These findings were confirmed by morphological analyses revealing that VLPs were densely bundled and accumulated on the surfaces of VLP-producing cells cultured in the presence of AGP127-8 and MGP72-17. Here, we discuss a novel mechanism of antibody-mediated inhibition of virus

95 infectivity that differs from “classical” neutralizing activity.

96

Materials and Methods

Viruses and cells. MARV strain Angola (51) was propagated in Vero E6 cells (kindly provided by Dr. R. Baric, University of North Carolina, Chapel Hill, NC, USA) and stored at -80°C until use. All infectious work with MARV was performed in the biosafety level 4 laboratories at the Integrated Research Facility in the Rocky Mountain Laboratories, Division of Intramural Research, National Institute of Allergy and Infectious Diseases, National Institute of Health, Hamilton, Montana, USA. Replication-incompetent vesicular stomatitis virus (VSV) pseudotyped with MARV (Angola) GP expressing green fluorescent protein was generated as described previously (40). A neutralizing MAb to VSV G protein, VSV-G(N)1-9 (24), was used to abolish the background infectivity of parental VSV bearing VSV G protein. The infectious unit (IU) of VSV bearing MARV GP was determined by counting the number of Vero E6 cells expressing green fluorescent protein under a fluorescent microscope. Vero E6 and Human embryonic kidney 293T (HEK293T) cells (3) were grown in Dulbecco's modified Eagle's medium. Mouse myeloma P3-U1 cells and hybridoma cell lines were maintained in Roswell Park Memorial Institute 1640 medium. The media were supplemented with fetal calf serum and antibiotics.

Monoclonal antibodies. MARV GP-specific MAbs, AGP2-1 (IgG1), AGP126-15 (IgG1), AGP127-8 (IgG1), AΔM16-2-13 (IgM), and MGP72-17 (IgM), were generated as described previously (24). Briefly, HEK293T cells were transfected with plasmids encoding MARV GP and VP40. VLPs produced and released in the supernatant were purified by ultracentrifugation through a 25% sucrose cushion. Five-week-old female BALB/c mice were intramuscularly and subcutaneously immunized with 150 μg of VLP for 3 times at 3-week intervals. Three weeks after the last immunization, mice were boosted intraperitoneally with 150 μg of VLPs. Three days later, spleen cells from these mice were fused with P3-U1 cells and maintained according to a standard procedure (32). Hybridomas were screened for secretion of MARV GP-specific MAbs by

enzyme-linked immunosorbent assay (ELISA) using purified C-terminal histidine-tagged MARV GP as an antigen (25), and hybridoma producing MAbs were cloned by limiting dilution of the cells. The isotypes of the obtained MAbs were determined using a mouse MAb isotyping test kit (AbD Serotec) according to the manufacturer's instructions. Protein A agarose columns (Bio-Rad) and KAPTIVE-M (Tecnogen) were used to purify monoclonal IgG and IgM, respectively from mouse ascites. H5-61-2-1 (IgG1) and APH159-1-3 (IgM) specific to influenza A virus hemagglutinins were used as irrelevant control antibodies. AGP2-1 (IgG1), whose epitope is different from that of AGP127-8 (24), and MVP40 1-17-1 specific for MARV VP40 were conjugated with Alexa Fluor 488 and 647, respectively, by using Zenon Mouse IgG1 Labeling Kits (Invitrogen) for immunofluorescence analysis (see below). Animal studies were carried out in strict accordance with the Guidelines for Proper Conduct of Animal Experiments of the Science Council of Japan. The protocol was approved by the Hokkaido University Animal Care and Use Committee. All efforts were made to minimize suffering.

Purification of AGP127-8 fragment antigen-binding (Fab). Purified AGP127-8 was digested by papain and the Fab fractions were yielded through ion-exchange chromatography using diethylethanolamine (TOYOPEARL DEAE-650M, Tosoh Corporation). Following solvent displacement with 10 mM sodium phosphate (pH 6.8), the samples containing Fab were fractionated through gel filtration chromatography (TSKgel G3000SW, Tosoh Corporation) and the Fab fraction was subjected to solvent displacement with phosphate-buffered saline (PBS) and concentrated by ultrafiltration (molecular weight cutoff 10 K).

Detection of MARV particles and VLPs released into culture media. Vero E6 cells grown in 12-well plates were inoculated with MARV at a multiplicity of infection (MOI) of 1.0 and cultured at 37°C with medium containing 50, 10, or 2 μg/ml of MAbs or in the absence of MAbs. At 24, 48,

147 72, and 96 hours postinoculation (hpi), supernatants were harvested and cleared of cell debris.
148 Samples were directly analyzed by sodium dodecyl sulfate-polyacrylamide gel electrophoresis
149 (SDS-PAGE) and western blotting. For VLP assays, HEK293T cells grown in 24-well plates were
150 cotransfected with the mammalian expression plasmid pCAGGS encoding MARV GP
151 (pC-AngolaGP), VP40 (pC-AngolaVP40), and NP (pC-AngolaNP) and maintained in medium
152 containing 50, 10, or 2 μg/ml of the respective MAbs or AGP127-8 Fab. At 48 hours
153 posttransfection, supernatants were collected and cleared from cell debris. Pellets and cells were
154 treated with lysis buffer (0.1 M Tris-HCl (pH7.5), 0.1 M NaCl, 1% Nonident P-40, 1% Triton
155 X-100, and Complete mini protease inhibitor (Roche)) and centrifuged to remove insoluble
156 fractions. Supernatants and cell lysates were subjected to SDS-PAGE and western blotting.
157
158 **Neutralization tests.** Serial dilutions of MAbs were prepared in Dulbecco's modified Eagle's
159 medium supplemented with 2% fetal bovine serum and 25 μl was incubated with 200 focus
160 forming units of MARV in a total volume of 50 μl. After 30 minutes at 37ºC, the MAb-virus
161 mixture was used to inoculate to Vero E6 cells seeded in a 48-well plate, and cells were incubated
162 for 60 minutes at 37ºC. Next, the mixture was removed from the cells and 0.5 ml of a 1.2%
163 carboxymethyl cellulose/MEM (Life Technologies) solution was added to each well. Following
164 incubation for 4 days at 37ºC, the plates were fixed with 10% neutral buffered formalin.
165 Subsequently, the cells were permeabilized and foci were stained with anti-MARV NP rabbit serum
166 produced by immunization with a synthetic peptide corresponding to amino acid residues 591-605
167 (GDILEPIRSPSSPSA) of the MARV Angola strain, designated FS0609, followed by an
168 fluorescein isothiocyanate-labeled secondary antibody (Sigma) as described previously (21). Foci
169 were counted using a fluorescent microscope. The neutralization test for pseudotyped VSV was
170 done as described previously (37). Briefly, VSVs pseudotyped with MARV GP ($10^{4.5}$ IU/ml) were
171 mixed with each appropriately diluted MAb, incubated for 1 hour at room temperature and

inoculated into confluent Vero E6 cells grown in 96-well plates. At 18 hpi, infectivity was determined by counting fluorescent cells. The relative percentage of infectivity was calculated by setting the number of cells infected in the absence of GP-specific MAbs to 100%.

SDS-PAGE and western blotting. Samples were analyzed by 7.5% SDS-PAGE and western blotting, as mentioned elsewhere (25). Briefly, cell culture supernatants or cell lysates were mixed with SDS-PAGE sample buffer with 5% 2-mercaptoethanol and heated for 5 minutes at 98°C. After electrophoresis, separated proteins were blotted on a polyvinylidene difluoride membrane (Millipore). FS0609 and a mouse monoclonal anti-β-actin antibody (AC-15; Abcam) were used as primary antibodies to detect MARV NP and β-actin, respectively. The bound antibodies were detected with peroxidase-conjugated AffiniPure donkey anti-rabbit IgG (H+L) (Jackson ImmunoResearch) and goat anti-mouse IgG (H+L) (Jackson ImmunoResearch), followed by visualization with Immobilon Western (Millipore).

ELISA. The filovirus GP-based ELISA was performed as described previously (25). Briefly, ELISA plates (Nunc Maxisorp) were coated with purified soluble MARV GP lacking the transmembrane domain (100 ng/50 μl/well), followed by blocking with 3% skim milk (200 μl/well). Appropriately diluted cultured media of hybridomas or purified MAbs were prepared, added to the ELISA plates and incubated for 1 hour at room temperature. Bound antibodies were visualized by adding secondary peroxidase-conjugated goat anti-mouse IgG and 3,3',5,5'-tetramethylbenzidine (Sigma). The reaction was stopped by adding 1 N sulfuric acid to the mixture, and the optical density at 450 nm was measured.

Immunofluorescence microscopy. HEK293T cells grown on a glass chamber slide were transfected with pC-AngolaGP, pC-AngolaVP40, and pC-AngolaNP or an equivalent quantity of

197 an empty vector (pCAGGS), and maintained in the presence (50 μg/ml) or absence of MAbs. At 24
198 hours posttransfection, cells were fixed with 4% paraformaldehyde for 30 minutes. Following
199 removal of the fixative, remaining aldehydes were quenched with 100 mM glycine in PBS. After
200 washing with PBS, cells were permeabilized with 0.1% Triton X-100 in PBS and incubated in
201 blocking solution (2% bovine serum albumin, 0.2% Tween 20, 5% glycerol, and 0.05% sodium
202 azide in PBS). GP and VP40 were stained with AGP2-1 conjugated with Alexa Fluor 488 and
203 MVP40 1-17-1 conjugated with Alexa Fluor 647, respectively. NP was detected with FS0609 and
204 goat anti-rabbit IgG conjugated with Alexa Fluor 405 (Invitrogen). After staining, samples were
205 fixed with 4% paraformaldehyde for 15 minutes. Fluorescent images were acquired using LSM
206 780 (Zeiss).
207
208 **Electron microscopy.** Transmission electron microscopy (TEM) and scanning electron
209 microscopy (SEM) were carried out as described previously (27, 47). For ultrathin-sections, 48
210 hours after transfection of HEK293T cells with pC-AngolaGP and pC-AngolaVP40, the cells were
211 fixed for 20 minutes with 2.5% glutaraldehyde in 0.1 M cacodylate buffer (pH 7.4). Cells were
212 scraped off the 12-well plate, pelleted by low-speed centrifugation, and then fixed for 30 minutes
213 with the same fixative. Small pieces of the fixed pellet were washed with cacodylate buffer,
214 postfixed with 2% osmium tetroxide in the cacodylate buffer for 1 hour at 4°C, dehydrated with a
215 series of ethanol gradients followed by propylene oxide, embedded in Epon 812 Resin mixture
216 (TAAB), and polymerized at 60°C for 2 days. Thin sections were stained with uranyl acetate and
217 lead citrate and examined with a TECNAI F20 electron microscope at 200 kV. For SEM, HEK293
218 cells transfected with pC-AngolaGP and pC-AngolaVP40 were fixed at 48 hours posttransfection.
219 The fixed cells were dehydrated with a series of ethanol gradients, substituted with t-butanol, and
220 dried in a Hitachi ES-2030 freeze dryer. Dried specimens were coated with osmium tetroxide by

using an HPC-1S osmium coater (Vacuum Device Inc.) and examined with a Hitachi S-4200 microscope.

Results

MARV GP-specific MAbs that inhibit virus release from infected cells. In a virus-neutralizing test, infectious viruses are generally mixed with antibodies prior to inoculation onto cultured cells and the reduction of infectivity is estimated by plaque counts or cytopathic effects. However, in the assay applied here, MARV was first inoculated onto Vero E6 cells at an MOI of 1 without preincubation with MAbs and then cultured in the media containing MAbs. The amounts of virus particles released into the culture supernatants were estimated by detecting virion-associated NP in western blotting. This assay enabled us to evaluate the ability of MAbs to inhibit the production of virus particles from infected cells in a single replication cycle of MARV infection. We tested 4 murine MARV GP-specific MAbs, AGP126-15 (IgG1), AGP127-8 (IgG1), AΔM16-2-13 (IgM), and MGP72-17 (IgM) in regard to their inhibitory activities for MARV particle production (Fig. 1).

In the absence of MAbs, NP was detected in the culture supernatants at 48 hpi and the NP signal was increased in a time-dependent manner, indicating increased virus release from infected cells over time. Similarly, NP was detected in the supernatants of cells maintained in the presence of a negative control MAb, APH159-1-3. AGP126-15 and AΔM16-2-13 only slightly reduced the amount of NP in the supernatants. By contrast, AGP127-8 and MGP72-17 showed remarkable inhibitory effects on virus release. In the presence of 10 or 50 μg/ml of MGP72-17, NP was almost undetectable in the supernatant collected at 48 hpi, and the intensity of the NP bands was obviously lower than those seen in the presence of the control MAb up to 96 hpi. Most surprisingly, NP was hardly detected over 96 hpi in the presence of AGP127-8 even at the lowest concentration tested (2 μg/ml).

Absence of neutralizing activity of MAbs AGP127-8 and MGP72-17. To clarify whether these antibodies have overlapping potential with neutralizing activity that blocks virus entry into host cells, the MAbs were assessed with an traditional neutralization test using VSV pseudotyped with

MARV GP (Figs. 2A and 2B). We found that neither of the GP-specific IgG MAbs (AGP126-15 and AGP127-8) tested showed neutralizing activity, although the IgM MAbs (AΔM16-2-13 and MGP72-17) minimally neutralized at high concentrations (Fig. 2B). Similarly, the infectivity of authentic MARV was not reduced by these MAbs in the neutralization test (Fig. 2C). Importantly, AGP127-8, which almost completely inhibited MARV release from infected cells (Fig. 1), showed no neutralizing activity. Taken together, these results indicate that the "classical" neutralizing activity of MAbs is not required to inhibit extracellular release of virus particles.

Inhibition of VLP formation by AGP127-8 and MGP72-17. Since AGP127-8 and MGP72-17, which do not block GP-mediated entry of MARV into host cells, drastically reduced the release of progeny viruses, we assume that AGP127-8 and MGP72-17 inhibit virus budding. To directly verify this hypothesis, we utilized a simple VLP formation assay. HEK293T cells were cotransfected with the mammalian expression plasmid pCAGGS encoding MARV GP, VP40, and NP and the amounts of NP incorporated into extracellular VLPs or accumulated in cells were estimated by western blotting (Fig. 3). Consistent with the results shown in figure 1, AGP127-8 and MGP72-17 significantly reduced the VLP formation in a dose-dependent manner, whereas AGP126-15 and AΔM16-2-13 did not remarkably alter the amounts of NP detected in the supernatants compared to control MAbs H5-61-2-1 and APH159-1-3 (Figs. 3A and 3B). Interestingly, the NP amounts were increased reciprocally in the lysates of VLP-producing cells incubated in the presence of AGP127-8 or MGP72-17, suggesting cellular accumulation of NP due to the decreased extracellular VLP release. AGP127-8 exhibited the highest budding-inhibition activity among the tested MAbs. VLP release of other MARV strain (Musoke) was also reduced by AGP127-8 and MGP72-17 (data not shown). Neither AGP127-8 nor MGP72-17 inhibited budding of VLPs composed of MARV VP40 and NP (data not shown). Taken together, these data suggest

that AGP127-8 and MGP72-17 inhibit VLP egress from cells, most likely by interfering with the budding process mediated by VP40 and GP.

To evaluate whether the multivalent binding of the IgG variable regions is of significance in regard to budding-inhibition capacity, the potential of AGP127-8 Fab was assessed in comparison to that of intact AGP127-8 IgG (Fig. 3C). Interestingly, the NP amount detected in the presence of AGP127-8 Fab was comparable to that in the control supernatant (i.e., without MAb) and NP accumulation was not observed in the cells. These results indicate that the bivalency of IgG binding to multiple GP molecules is essential for the inhibition of VLP formation.

Localization of GP, VP40, and NP in VLP-producing cells. To further investigate the mechanisms by which AGP127-8 and MGP72-17 reduce the budding efficiency, HEK293T cells transfected with GP-, VP40-, and NP-expressing plasmids were cultured with or without these MAbs and examined by confocal microscopy (Fig. 4). Distribution of GP, VP40, and NP in the cells was separately visualized by multiple staining with Alexa Fluor. In the absence of MAbs, numerous filamentous structures accompanied by GP, VP40, and NP, some of which were most likely filopodia (15), protruded from the cell surface. Similar filamentous structures were observed in the cells treated with control MAbs AGP126-15 and AΔM16-2-13, although the filamentous protrusions were slightly shortened (Fig. 4). By contrast, when transfected cells were cultured in the presence of AGP127-8 or MGP72-17, these viral proteins were colocalized but accumulated mainly along smooth cell surfaces with few protruding filamentous structures. Since the overall expression levels and distribution of the GP, VP40, and NP in the cells did not seem to be altered by AGP127-8 and MGP72-17, diminished elongation of filamentous structures might be associated with impaired VLP release in the presence of these MAbs.

We then examined the distribution of AGP127-8 itself in HEK293T cells expressing GP, VP40, and NP, since uptake of virus-specific antibodies bound to viral proteins expressed on the

cells was reported for human cytomegalovirus-infected cells (20) and therefore it might be possible that AGP127-8 bound to GP was introduced into cells and negatively affected the VLP formation intracellularly. However, AGP127-8 was only detected on the surfaces of cells expressing GP, VP40, and NP (Fig. S1), indicating that AGP127-8 inhibited VLP formation extracellularly.

Cell surface morphology of VLP-producing cells in electron microscopy. To gain insight into the mechanism of antibody-mediated inhibitory effects on the MARV budding process, we examined HEK293T cells expressing GP and VP40 using TEM and SEM. We found that cells cultured without MAbs produced filamentous VLPs budding from the cell surface (Figs. 5A, 5D, and 5G), as reported previously (27). In the absence of MAbs, numerous filamentous prominences were observed on the cell surface (Figs. 5D and 5G), consistent with the immunocytochemical analyses shown in figure 4. Similar VLP formation was found in the cells treated with control MAbs AΔM16-2-13 or AGP126-15 (Fig S3). By contrast, VLPs were not released efficiently from cells in the presence of AGP127-8 and MGP72-17 (Figs. 5B and 5C), and appeared to be tangled and piled up on the cell surface (Figs. 5E, 5F, 5H, and 5I). Abnormal accumulation of filamentous structures, most likely unformed VLPs that were not pinched off from the cell membrane, was also found in ultrathin sections of the cells cultured with AGP127-8 or MGP72-17 (Figs. 5B and 5C). These data suggest that AGP127-8 and MGP72-17 bundle filamentous VLPs on the cell surface during the budding process (Figs. 5E, 5F, 5H, and 5I).

Discussion

In general, neutralizing antibodies recognize epitopes on viral surface proteins and block essential steps for invasion of viruses into host cells such as attachment to viral receptors and fusion of the viral envelope with the plasma membrane. Several MAbs to EBOV GP, for example KZ52, ZGP133/3.16, and JP3K11, have been shown to neutralize EBOV effectively *in vitro*, by inhibiting the cellular entry pathway of the virus (16, 17, 33, 37, 38). In contrast, there has been no report demonstrating an effective neutralizing MAb against MARV. However, it was recently shown that passive immunization of nonhuman primates with antibodies was fully protective against lethal MARV and EBOV infection (4, 29), suggesting the pivotal role of antibodies in protective immunity. In the present study, we propose a novel mechanism by which antibodies counteract MARV particle budding.

We found that the budding and extracellular release of MARV were inhibited by MAbs AGP127-8 and MGP72-17 (Fig. 1), whereas these MAbs did not display "classical" neutralizing activity (Fig. 2). Morphological analyses by electron microscopy suggested that AGP127-8 and MGP72-17 deposited a tremendous number of unreleased VLPs on the cell surface (Fig. 5). On the other hand, the AGP127-8 Fab did not inhibit VLP budding (Fig. 3C), indicating that multiple antigen-binding sites of the intact IgG are a prerequisite for the budding-inhibition activity. Thus, the most plausible explanation for the mechanism underlying the inhibitory effects of these GP-specific MAbs on virus particle budding is that the antibodies crosslink multiple GP molecules expressed on the infected cell surface before initiation of the budding process and, consequently, this intricate cross-linkage via antibodies and GPs mechanically interferes with the driving force for MARV budding, resulting in the accumulation of premature and unreleased virus particles on the cells.

It might also be possible that the interaction between antibodies and cell surface GPs causes intracellular signaling against viral protein transport and/or assembly. It has been shown

342 that VP40 is the key factor for filovirus assembly and budding, which require its interaction with
343 host proteins (19). The majority of MARV VP40 is transported to the cell surface along with GP
344 through a retrograde endosomal pathway by hijacking the ESCRT machinery of the cells, and
345 newly assembled virions are finally released from host cells (9, 13, 14, 43, 44). Thus, such cellular
346 machinery utilized for assembly and budding of MARV might be affected by intracellular signaling
347 via the interaction between GP-specific antibodies and GPs on the cell surface. There are indeed
348 several examples of such a phenomenon (e.g., varicella-zoster or measles virus infection) in which
349 the binding of virus-specific antibodies to viral proteins expressed on the cell surface suppressively
350 modulates distribution and synthesis patterns of viral proteins in infected cells (7, 8, 31, 34, 52).
351 Interestingly, inhibition of MARV budding by AGP127-8 was not simply dependent on its
352 affinity to GP, since AGP127-8 and AGP126-15 showed similar binding capacities to GPs (Fig. S3)
353 whereas a remarkable difference in the budding-inhibition activities was seen between these MAbs.
354 This indicates that the epitopes of these MAbs are likely the critical factor for the inhibitory
355 activity. Both AGP127-8 and AGP126-15 recognize epitopes (amino acid positions 411-430 and
356 369-385, respectively) located in the mucin-like region of GP (24). The mucin-like region plays an
357 important role in attachment to the preferred target cells (e.g., hepatocytes, endothelial cells,
358 dendritic cells, and macrophages), whose infection is likely involved in filovirus pathogenesis (36).
359 Importantly, however, the mucin-like region is not essential for the fundamental function of GP in
360 viral entry into cells *in vitro* (22, 35, 39), and thus is unlikely to contain important epitopes for
361 neutralizing antibodies. On the other hand, our data suggest that some antibodies recognizing
362 epitopes on the mucin-like region, such as AGP127-8, have a strong activity to inhibit MARV
363 budding, which leads to reduced production of progeny viruses. It is noted that the epitope of
364 AGP127-8 is located near the furin cleavage site at the C-terminus of GP1 which is likely
365 unexposed on the uncleaved GP molecules (Fig. S4). Thus, it can be hypothesized that the

C-terminus of cleaved GP1 might have some biological functions to facilitate extracellular virus release.

The present study proposes a novel mechanism of antibody-mediated inhibition of MARV infection. It would be of interest to investigate whether certain EBOV GP-specific MAbs also have a similar capacity to inhibit the process of virus budding. It should be noted that passively transferred anti-EBOV GP nonneutralizing MAbs recognizing epitopes in the mucin-like region were protective in a mouse model of lethal EBOV infection (49). As evidenced by the well-known efficacy of influenza virus neuraminidase inhibitors, the viral budding process is a promising target for antiviral development. Our data lead to the idea that the "classical" neutralizing activity is not the only indicator of protective antibody and MAbs like AGP127-8 may have the potential for prophylactic and therapeutic use. Recent reports demonstrated that antibody therapy is a promising strategy for treating filovirus infection (4, 21, 29). Furthermore, a detailed analysis of the precise mechanism by which MAbs interfere with the virus budding process may provide new insights into the development of prophylactic and therapeutic measures against virus infections.

Acknowledgments

We thank Hiroko Miyamoto, Ayaka Yokoyama, Kazumasa Yokoyama, Dr. Manabu Igarashi (Hokkaido University Research Center for Zoonosis Control), and Dr. Hideki Ebihara (National Institute of Allergy and Infectious Diseases, National Institutes of Health, Rocky Mountain Laboratories) for technical assistance or valuable advice, and Kim Barrymore for editing the manuscript.

This work was supported by the Japan Initiative for Global Research Network on Infectious Diseases (J-GRID), the Global COE Program, a Grant-in-Aid from the Ministry of Education, Culture, Sports, Science and Technology (MEXT), ERATO (Japan Science and Technology Agency), and National Institute of Allergy and Infectious Disease Public Health Service research grants. Funding was also provided by a Grant-in-Aid from the Ministry of Health, Labour and Welfare of Japan, and by the Division of Intramural Research, National Institute of Allergy and Infectious Diseases, National Institutes of Health, USA.

References

1. **Corboba P, Grutadauria S, Cuffini C, Zapata M.** 2000. Neutralizing monoclonal antibody to the E1 glycoprotein epitope of rubella virus mediates virus arrest in VERO cells. Viral Immunol. **13:** 83-92.
2. **Driscoll DM, Onuma M, Olson C.** 1977. Inhibition of bovine leukemia virus release by antiviral antibodies. Arch. Virol. **55:** 139-144.
3. **DuBridge RB, Tang P, Hsia HC, Leong PM, Miller JH, Calos MP.** 1987. Analysis of mutation in human cells by using an Epstein-Barr virus shuttle system. Mol. Cell Biol. **7:** 379-387.
4. **Dye JM, Herbert AS, Kuehne AI, Barth JF, Muhammad MA, Zak SE, Ortiz RA, Prugar LI, Pratt WD.** 2012. Postexposure antibody prophylaxis protects nonhuman primates from filovirus disease. Proc. Natl. Acad. Sci. U. S. A. **109:** 5034-5039.
5. **Feldmann H, Nichol ST, Klenk HD, Peters CJ, Sanchez A.** 1994. Characterization of filoviruses based on differences in structure and antigenicity of the virion glycoprotein. Virology **199:** 469-473.
6. **Feldmann H, Will C, Schikore M, Slenczka W, Klenk HD.** 1991. Glycosylation and oligomerization of the spike protein of Marburg virus. Virology **182:** 353-356.
7. **Fujinami RS, Norrby E, Oldstone MB.** 1984. Antigenic modulation induced by monoclonal antibodies: antibodies to measles virus hemagglutinin alters expression of other viral polypeptides in infected cells. J. Immunol. **132:** 2618-2621.
8. **Fujinami RS, Oldstone MB.** 1980. Alterations in expression of measles virus polypeptides by antibody: molecular events in antibody-induced antigenic modulation. J. Immunol. **125:** 78-85.
9. **Harty RN.** 2009. No exit: targeting the budding process to inhibit filovirus replication. Antiviral Res. **81:** 189-197.
10. **Harty RN, Brown ME, Wang G, Huibregtse J, Hayes FP.** 2000. A PPxY motif within the

VP40 protein of Ebola virus interacts physically and functionally with a ubiquitin ligase: implications for filovirus budding. Proc. Natl. Acad. Sci. U. S. A. **97:** 13871–13876.

11. **Jasenosky LD, Neumann G, Lukashevich I, Kawaoka Y.** 2001. Ebola virus VP40-induced particle formation and association with the lipid bilayer. J. Virol. **75:** 5205–5214.
12. **Johansson BE, Grajower B, Kilbourne ED.** 1993. Infection-permissive immunization with influenza virus neuraminidase prevents weight loss in infected mice. Vaccine **11:** 1037–1039.
13. **Kolesnikova L, Bamberg S, Berghöfer B, Becker S.** 2004. The matrix protein of Marburg virus is transported to the plasma membrane along cellular membranes: exploiting the retrograde late endosomal pathway. J. Virol. **78:** 2382-2393.
14. **Kolesnikova L, Berghöfer B, Bamberg S, Becker S.** 2004. Multivesicular bodies as a platform for formation of the Marburg virus envelope. J. Virol. **78:** 12277-12287.
15. **Kolesnikova L, Bohil AB, Cheney RE, Becker S.** 2007. Budding of Marburgvirus is associated with filopodia. Cell Microbiol. **9:** 939-951.
16. **Lee JE, Fusco ML, Hessell AJ, Oswald WB, Burton DR, Saphire EO.** 2008. Structure of the Ebola virus glycoprotein bound to a human survivor antibody. Nature **454:** 177-182.
17. **Lee JE, Saphire EO.** 2009. Neutralizing ebolavirus: structural insights into the envelope glycoprotein and antibodies targeted against it. Curr. Opin. Struct. Biol. **19:** 408-417.
18. **Licata JM, Johnson RF, Han Z, Harty RN.** 2004. Contribution of ebola virus glycoprotein, nucleoprotein, and VP24 to budding of VP40 virus-like particles. J. Virol. **78:** 7344-7351.
19. **Liu Y, Harty RN.** 2010. Viral and host proteins that modulate filovirus budding. Future Virol. **5:** 481-491.
20. **Manley K, Anderson J, Yang F, Szustakowski J, Oakeley EJ, Compton T, Feire AL.** 2011. Human cytomegalovirus escapes a naturally occurring neutralizing antibody by incorporating it into assembling virions. Cell Host Microbe **10:** 197-209.
21. **Marzi A, Yoshida R, Miyamoto H, Ishijima M, Suzuki Y, Higuchi M, Matsuyama Y,**

Igarashi M, Nakayama E, Kuroda M, Saijo M, Feldmann F, Brining D, Feldmann H, Takada A. 2012. Protective efficacy of neutralizing monoclonal antibodies in a nonhuman primate model of Ebola hemorrhagic fever. PLoS ONE **7:** e36192. doi:10.1371/journal.pone.0036192.

22. **Matsuno K, Kishida N, Usami K, Igarashi M, Yoshida R, Nakayama E, Shimojima M, Feldmann H, Irimura T, Kawaoka Y, Takada A.** 2010. Different potential of C-type lectin-mediated entry between Marburg virus strains. J. Virol. **84:** 5140–5147.

23. **Nakayama E, Takada A.** 2011. Ebola and Marburg Viruses. J. Disast. Res. **6:** 381-389.

24. **Nakayama E, Tomabechi D, Matsuno K, Kishida N, Yoshida R, Feldmann H, Takada A.** 2011. Antibody-dependent enhancement of Marburg virus infection. J. Infect. Dis. **204:** S978-S985.

25. **Nakayama E, Yokoyama A, Miyamoto H, Igarashi M, Kishida N, Matsuno K, Marzi A, Feldmann H, Ito K, Saijo M, Takada A.** 2010. Enzyme-linked immunosorbent assay for detection of filovirus species-specific antibodies. Clin. Vaccine Immunol. **17:** 1723-1728.

26. **Nayak B, Kumar S, DiNapoli JM, Paldurai A, Perez DR, Collins PL, Samal SK.** 2010. Contributions of the avian influenza virus HA, NA, and M2 surface proteins to the induction of neutralizing antibodies and protective immunity. J. Virol. **84:** 2408-2420.

27. **Noda T, Sagara H, Suzuki E, Takada A, Kida H, Kawaoka Y.** 2002. Ebola virus VP40 drives the formation of virus-like filamentous particles along with GP. J. Virol. **76:** 4855-4865.

28. **Orvell C, Kristensson K.** 1985. The effects of monoclonal antibodies against the hemagglutinin-neuraminidase and fusion protein on the release of Sendai virus from infected cells. Arch. Virol. **86:** 1-15.

29. **Qiu X, Audet J, Wong G, Pillet S, Bello A, Cabral T, Strong JE, Plummer F, Corbett CR, Alimonti JB, Kobinger GP.** 2012. Successful treatment of ebola virus-infected cynomolgus macaques with monoclonal antibodies. Sci. Transl. Med. **4:**138ra81.

30. **Sanchez A, Geisbert TW, Feldmann H.** 2007. Filoviridae: Marburg and Ebola viruses. p 1409-1448. *In* Knipe DM, Howley PM (ed), Fields Virology, 5th ed, vol 1. Lippincott Williams & Wilkins, a Wolters Kluwer Business. Philadelphia.

31. **Schneider-Schaulies S, Liebert UG, Segev Y, Rager-Zisman B, Wolfson M, ter Meulen V.** 1992. Antibody-dependent transcriptional regulation of measles virus in persistently infected neural cells. J. Virol. **66:** 5534-5541.

32. **Shahhosseini S, Das D, Qiu X, Feldmann H, Jones SM, Suresh MR.** 2007. Production and characterization of monoclonal antibodies against different epitopes of Ebola virus antigens. J. Virol. Methods **143:** 29-37.

33. **Shedlock DJ, Bailey MA, Popernack PM, Cunningham JM, Burton DR, Sullivan NJ.** 2010. Antibody-mediated neutralization of Ebola virus can occur by two distinct mechanisms. Virology **401:** 228-235.

34. **Shiraki K, Daikoku T, Takemoto M, Yoshida Y, Suzuki K, Akahori Y, Okuno T, Kurosawa Y, Asano Y.** 2011. Neutralizing anti-gH antibody of Varicella-zoster virus modulates distribution of gH and induces gene regulation, mimicking latency. J. Virol. **85:** 8172-8180.

35. **Simmons G, Wool-Lewis RJ, Baribaud F, Netter RC, Bates P.** 2002. Ebola virus glycoproteins induce global surface protein down-modulation and loss of cell adherence. J. Virol. **76:** 2518–2528.

36. **Takada A.** 2012. Filovirus tropism: cellular molecules for viral entry. Front. Microbiol. **3:** 34.

37. **Takada A, Ebihara H, Jones S, Feldmann H, Kawaoka Y.** 2007. Protective efficacy of neutralizing antibodies against Ebola virus infection. Vaccine **25:** 993-999.

38. **Takada A, Feldmann H, Stroeher U, Bray M, Watanabe S, Ito H, McGregor M, Kawaoka Y.** 2003. Identification of protective epitopes on ebola virus glycoprotein at the single amino acid level by using recombinant vesicular stomatitis viruses. J. Virol. **77:** 1069-1074.

39. **Takada A, Fujioka K, Tsuiji M, Morikawa A, Higashi N, Ebihara H, Kobasa D, Feldmann**

H, Irimura T, Kawaoka Y. 2004. Human macrophage C-type lectin specific for galactose and N-acetylgalactosamine promotes filovirus entry. J. Virol. **78:** 2943-2947.

40. **Takada A, Robison C, Goto H, Sanchez A, Murti KG, Whitt MA, Kawaoka Y.** 1997. A system for functional analysis of Ebola virus glycoprotein. Proc. Natl. Acad. Sci. U. S. A. **94:** 14764-14769.
41. **Timmins J, Scianimanico S, Schoehn G, Weissenhorn W.** 2001. Vesicular release of ebola virus matrix protein VP40. Virology **283:** 1-6.
42. **Towner JS, Amman BR, Sealy TK, Carroll SA, Comer JA, Kemp A, Swanepoel R, Paddock CD, Balinandi S, Khristova ML, Formenty PB, Albarino CG, Miller DM, Reed ZD, Kayiwa JT, Mills JN, Cannon DL, Greer PW, Byaruhanga E, Farnon EC, Atimnedi P, Okware S, Katongole-Mbidde E, Downing R, Tappero JW, Zaki SR, Ksiazek TG, Nichol ST, Rollin PE. 2009.** Isolation of Genetically Diverse Marburg Viruses from Egyptian Fruit Bats. PLoS Pathog. **5:** e1000536. doi:10.1371/journal.ppat.1000536.
43. **Urata S, Noda T, Kawaoka Y, Morikawa S, Yokosawa H, Yasuda J.** 2007. Interaction of Tsg101 with Marburg virus VP40 depends on the PPPY motif, but not the PT/SAP motif as in the case of Ebola virus, and Tsg101 plays a critical role in the budding of Marburg virus-like particles induced by VP40, NP, and GP. J. Virol. **81:** 4895-4899.
44. **Urata S, Yasuda J.** 2010. Regulation of Marburg virus (MARV) budding by Nedd4.1: a different WW domain of Nedd4.1 is critical for binding to MARV and Ebola virus VP40. J. Gen. Virol. **91:** 228-234.
45. **Vanderplasschen A, Hollinshead M, Smith GL.** 1997. Antibodies against vaccinia virus do not neutralize extracellular enveloped virus but prevent virus release from infected cells and comet formation. J. Gen. Virol. **78:** 2041-2048.
46. **Volchkov VE, Volchkova VA, Ströher U, Becker S, Dolnik O, Cieplik M, Garten W, Klenk HD, Feldmann H.** 2000. Proteolytic processing of Marburg virus glycoprotein. Virology **268:**

1-6.

47. **Watanabe S, Watanabe T, Noda T, Takada A, Feldmann H, Jasenosky LD, Kawaoka Y.** 2004. Production of novel ebola virus-like particles from cDNAs: an alternative to ebola virus generation by reverse genetics. J. Virol. **78:** 999-1005.
48. **Webster RG, Reay PA, Laver WG.** 1988. Protection against lethal influenza with neuraminidase. Virology **164:** 230–237.
49. **Wilson JA, Hevey M, Bakken R, Guest S, Bray M, Schmaljohn AL, Hart MK.** 2000. Epitopes involved in antibody-mediated protection from Ebola virus. Science **287:** 1664-1666.
50. **Wool-Lewis RJ, Bates P.** 1998. Characterization of Ebola virus entry by using pseudotyped viruses: identification of receptor-deficient cell lines. J. Virol. **72:** 3155-3160.
51. **World Health Organization.** 2005. Marburg haemorrhagic fever, Angola. Wkly. Epidemiol. Rec. **80:** 158-159.
52. **Zinnheimer-Dreikorn J, Koschel KP.** 1990. Antigenic modulation of measles subacute sclerosing panencephalitis virus in a persistently infected rat glioma cell line by monoclonal anti-haemagglutinin antibodies. J. Gen. Virol. **71:** 1391-1394.

Figure legends

Figure 1. Detection of NP in the supernatants of cells infected with MARV. Vero E6 cells were infected with MARV at an MOI of 1.0. Following 1-hour incubation for virus adsorption, cells were cultured in the media containing 50, 10, or 2 μg/ml of GP-specific IgG (AGP126-15 and AGP127-8), IgM (AΔM16-2-13 and MGP72-17), an irrelevant negative control MAb (APH159-1-3), or without MAbs. Supernatants were collected every 24 hpi over 96 hpi. NP in virus particles released into the supernatants was detected by western blotting as described in Materials and Methods. Experiments were conducted three times and representative data are shown.

Figure 2. Neutralizing activity of MAbs. VSV pseudotyped with MARV GP was incubated with 5, 10, or 50 μg/ml of GP-specific IgG (A) or IgM MAbs (B) for 1 hour and subsequently inoculated into confluent Vero E6 cells. Neutralizing activity of MAbs was also tested for authentic MARV (C). H5-61-2-1 and APH159-1-3 were used as irrelevant negative control MAbs. Experiments using pseudotyped VSV (A and B) and MARV (C) were performed 3 and 2 times, respectively, and averages and standard deviations are shown.

Figure 3. Detection of VLPs in the supernatants of cells expressing GP, VP40, and NP. Subconfluent HEK293T cells were cotransfected with pC-AngolaGP, pC-AngolaVP40, and pC-AngolaNP, or empty pCAGGS (mock), and maintained with 50, 10, or 2 μg/ml of MAbs or without MAbs (A and B). At 48 hours posttransfection, supernatants and cell lysates were subjected to SDS-PAGE, followed by western blotting. The AGP127-8 Fab was also tested under the same conditions (C). Experiments were conducted three times and a representative data set is shown.

Figure 4. Immunofluorescence images of cells expressing GP, VP40, and NP in the presence of antibodies. HEK293T cells transfected with pC-AngolaGP, pC-AngolaVP40, and pC-AngolaNP

were incubated in the absence or presence of respective antibodies. GP and VP40 were probed using AGP2-1 conjugated with Alexa Fluor 488 and MVP40 1-17-1 conjugated with Alexa Fluor 647, respectively. NP was detected with the anti-NP rabbit serum FS0609 and goat anti-rabbit IgG antibody conjugated with Alexa Fluor 405. Low (A) and high (B) magnification images are shown with scale bars, 10 μm (A) and 2 μm (B).

Figure 5. TEM and SEM images of cells expressing GP and VP40 in the presence of AGP127-8 or MGP72-17. HEK293T cells transfected with pC-AngolaGP and pC-AngolaVP40 were incubated in the absence (A, D, and G) or presence of either AGP127-8 (B, E, and H) or MGP72-17 (C, F, and I). Ultrathin sections were examined under TEM (A-C). SEM images are shown at low (D-F) and high (G-I) magnification. Scale bars represent 500 nm (A-C), 10 μm (D-F), and 3 μm (G-I).

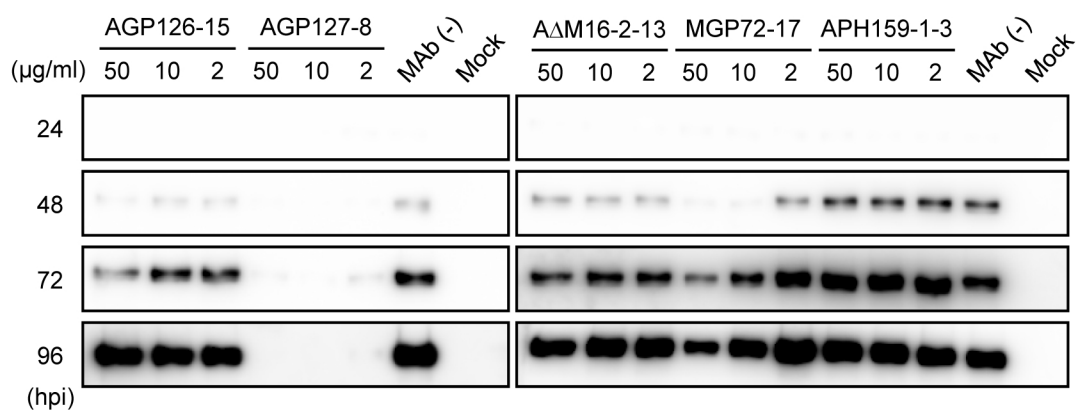


Figure 1 Kajihara *et al.*

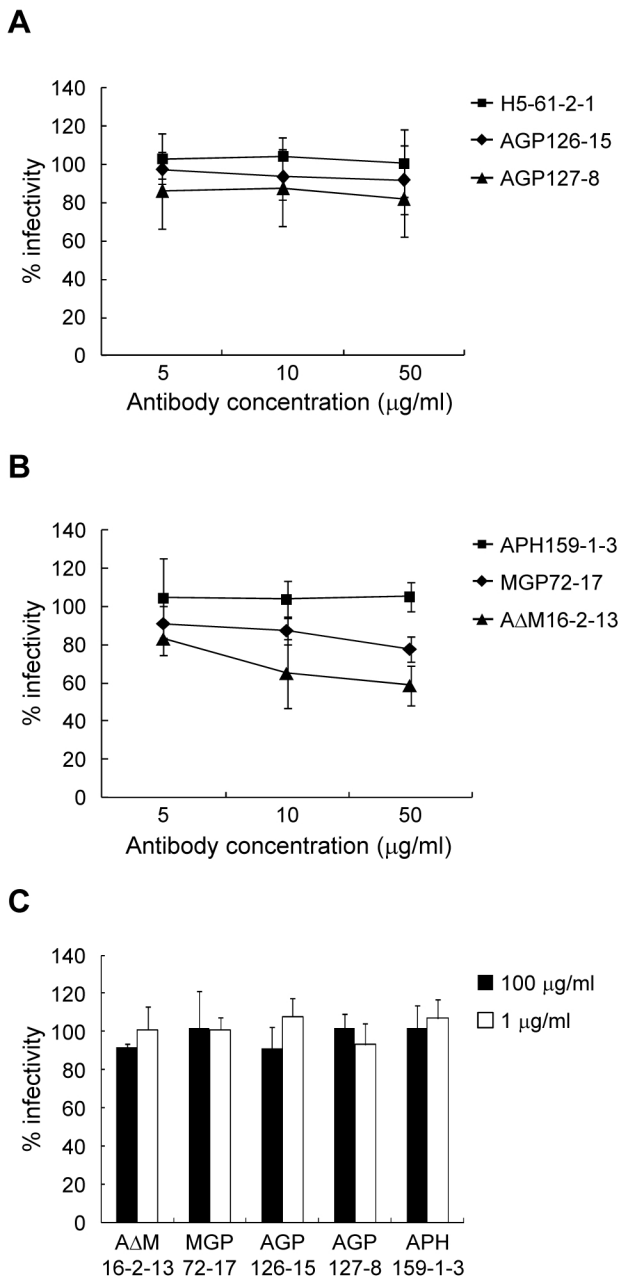


Figure 2 Kajihara *et al.*

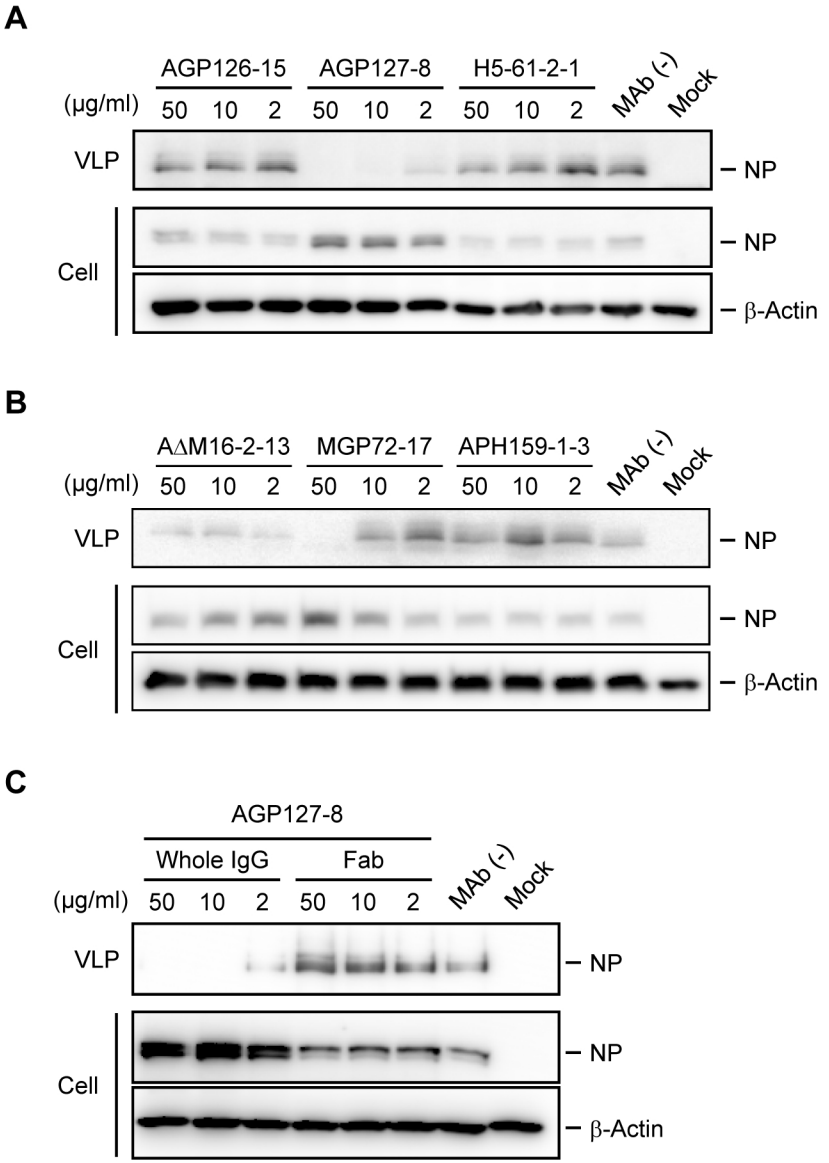


Figure 3 Kajihara *et al.*

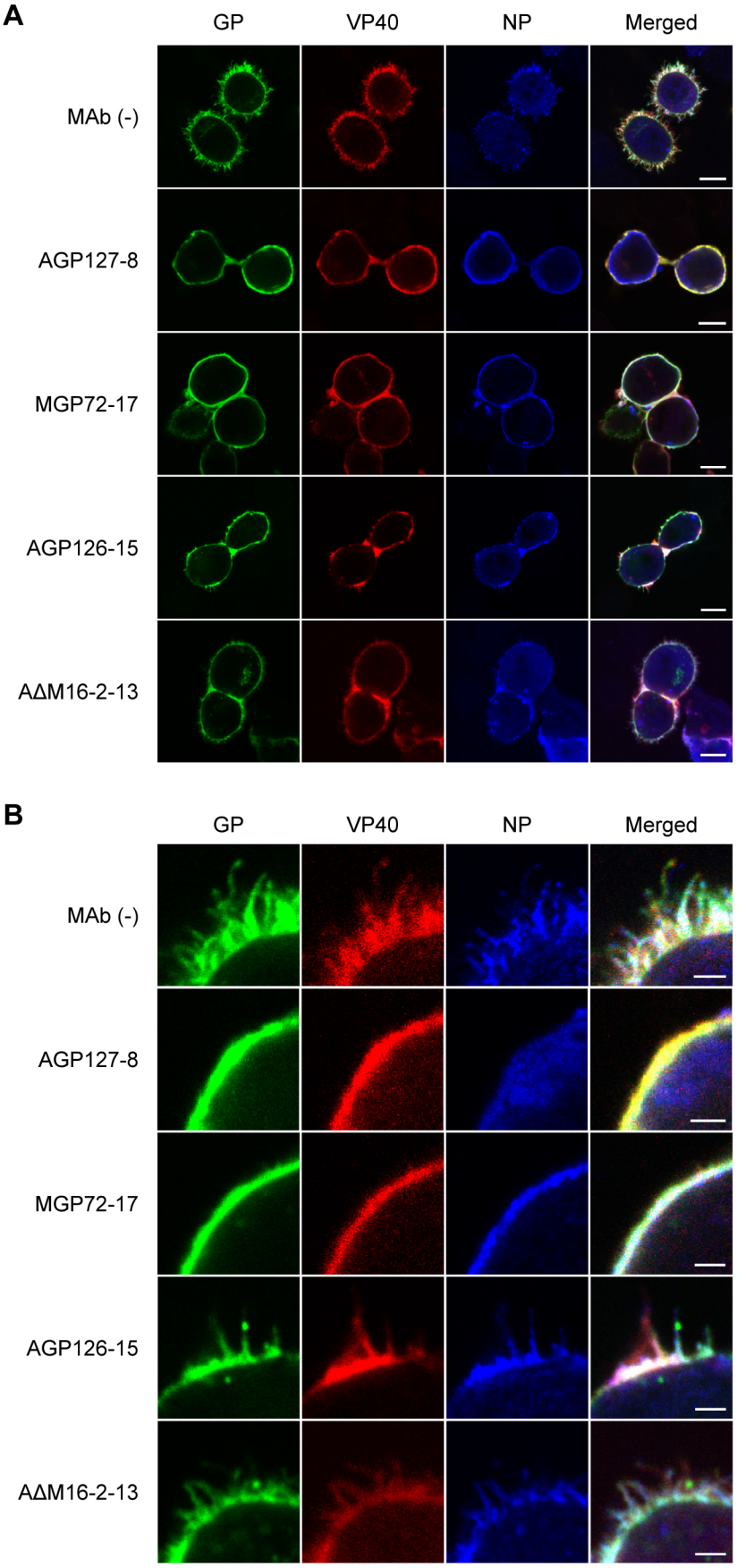


Figure 4
Kajihara *et al.*

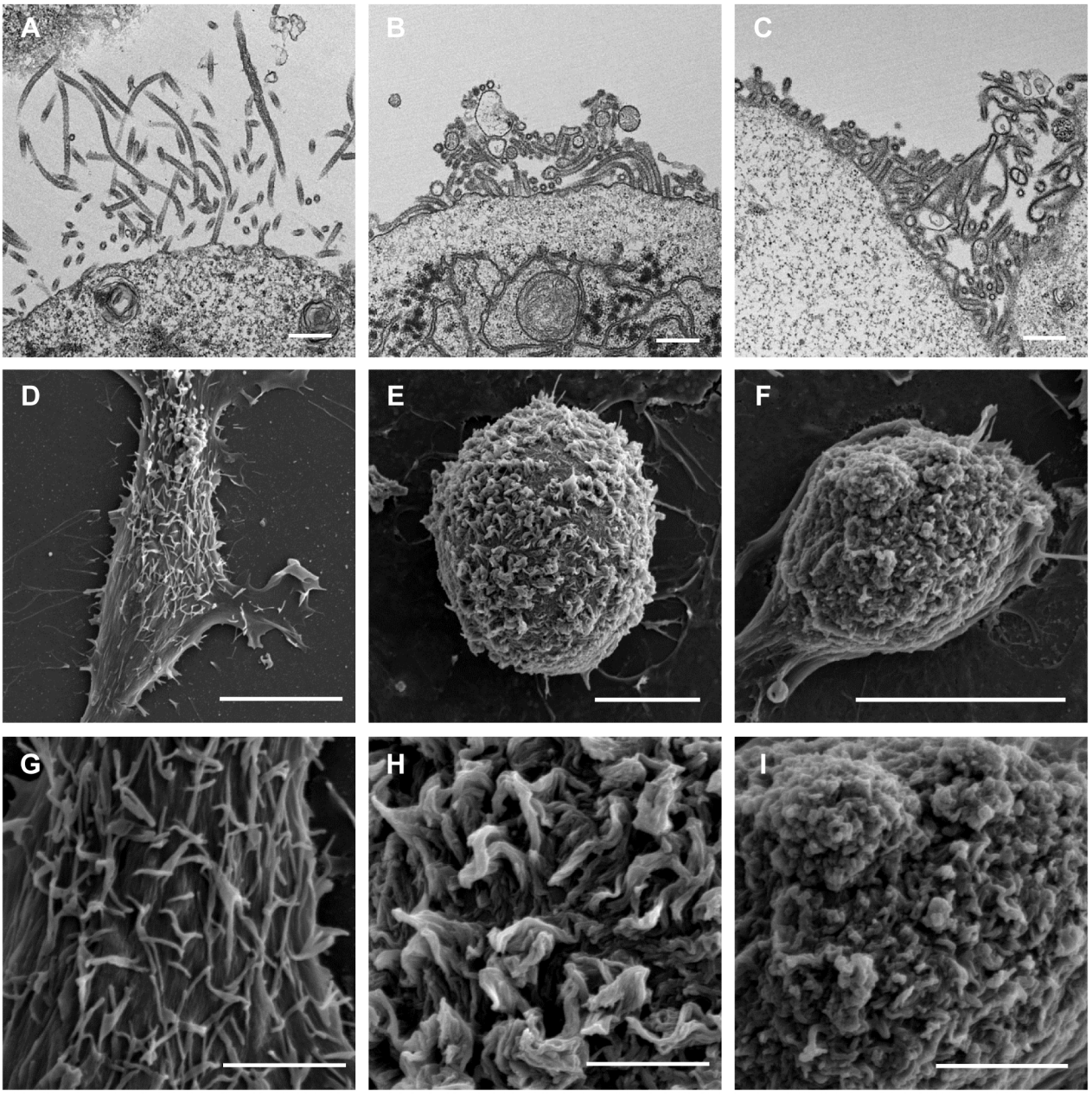


Figure 5 Kajihara *et al.*

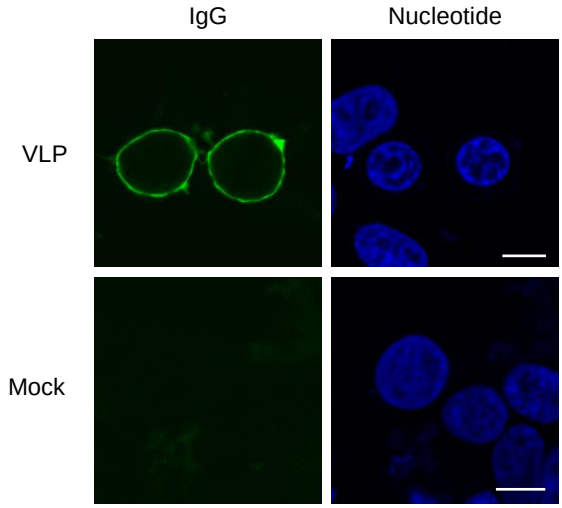


Figure S1. Distribution of AGP127-8 in cells expressing GP, VP40, and NP. HEK293T cells cotransfected with pC-AngolaGP, pC-AngolaVP40, and pC-AngolaNP, or empty pCAGGS (mock) were cultured in the presence of AGP127-8. 24 hours posttransfection, AGP127-8 was stained with goat anti-mouse IgG conjugated with Alexa Fluor 488. Nucleotides were also stained by DAPI. Scale bars represent 10 μm.

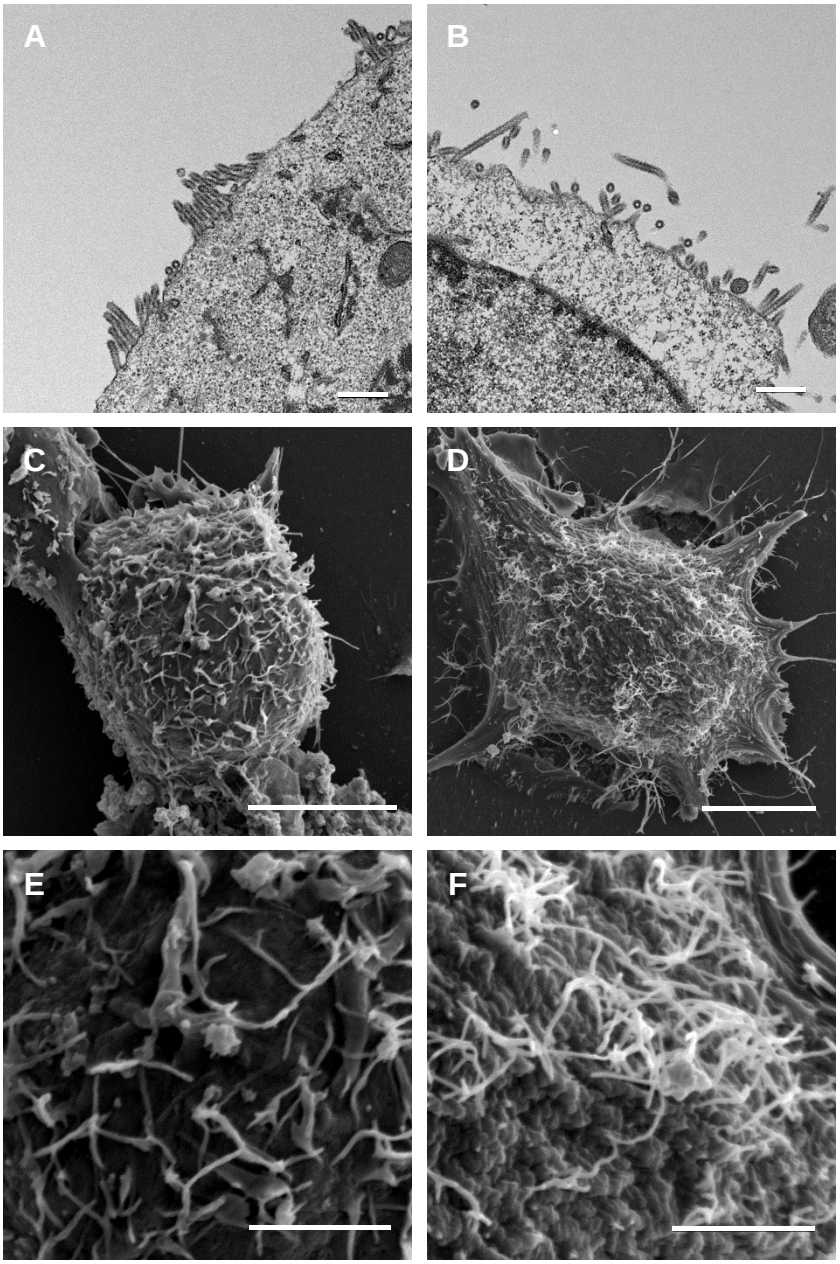


Figure S2. TEM and SEM images of cells expressing GP and VP40 in the presence of AGP126-15 or AΔM16-2-13. HEK293T cells transfected with pC-AngolaGP and pC-AngolaVP40 were incubated in the presence of AGP126-15 (A, C, E) or AΔM16-2-13 (B, D, F). Ultrathin sections were examined by TEM (A, B). SEM images are shown at low (C, D) and high (E, F) magnification. Scale bars represent 500 nm (A, B), 10 μm (C, D), and 3 μm (E, F).

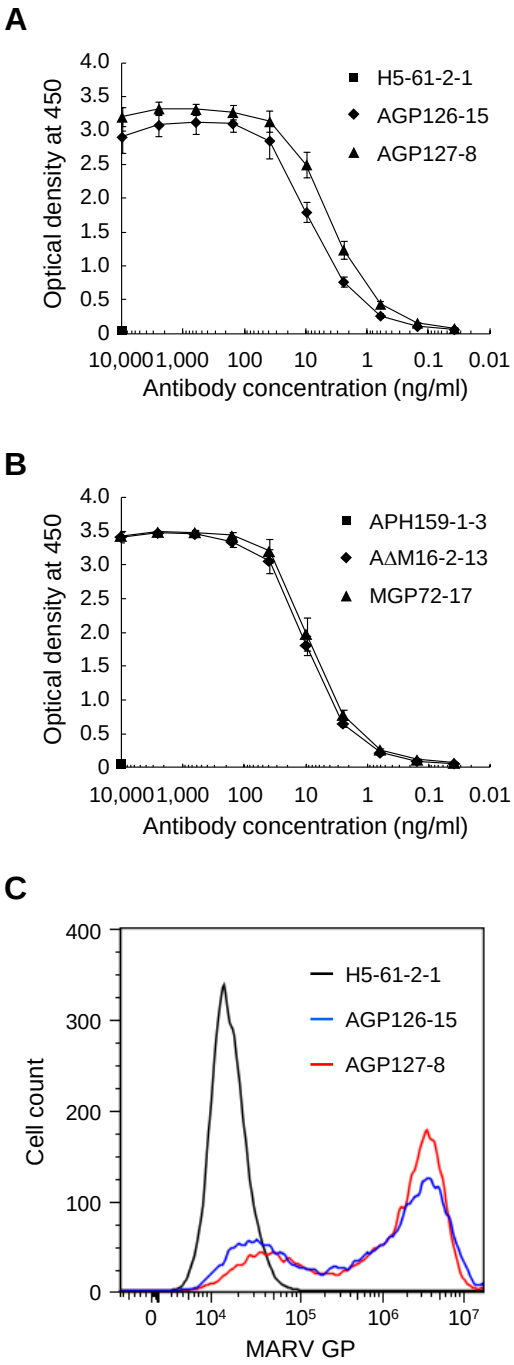


Figure S3. MAb binding capacity to MARV GP. MAb reactivities to soluble GP were measured by ELISA for IgG1 (A) and IgM (B) as described in Methods. H5-61-2-1 and APH159-1-3 were used as irrelevant negative control IgG1 and IgM antibodies, respectively. MAb binding to GP expressed on the cell surface was estimated by flow cytometry (C). HEK293T cells transfected with pC-AngolaGP were collected at 36 hours posttransfection and fixed with 4% paraformaldehyde. MARV GPs expressed on the cell surface were probed with 5 μg of GP-specific MAbs (AGP126-15 or AGP127-8) or a control MAb (H5-61-2-1) and bound MAbs were stained with goat anti-mouse IgG (H+L) conjugated with Alexa Fluor 488 (Invitrogen). Cells were then analyzed using BD FACSCanto II (Becton, Dickinson and Company).

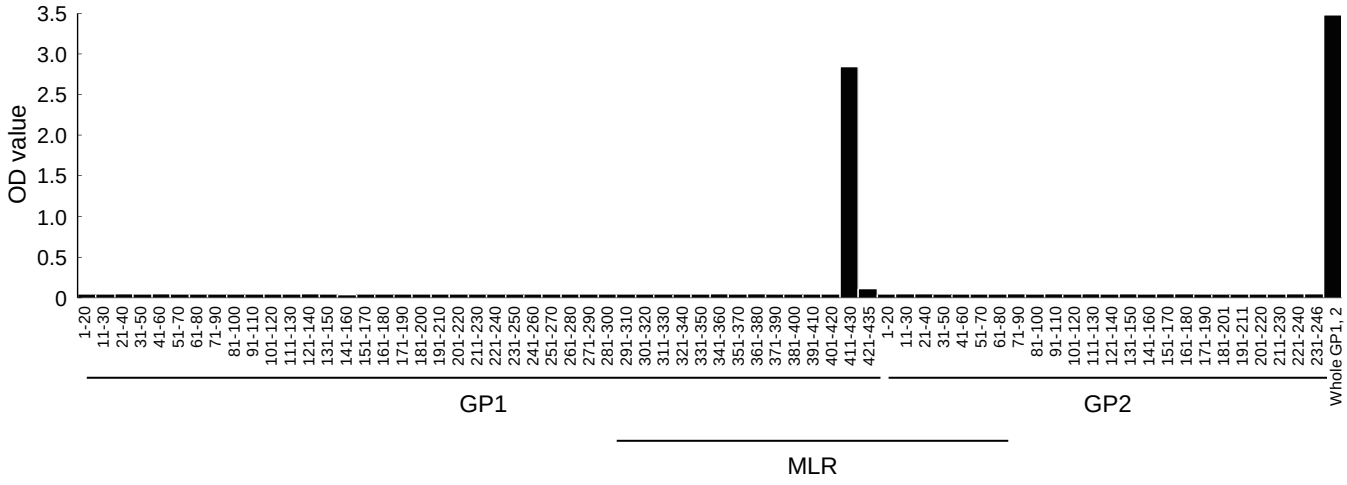


Figure S4. Identification of the AGP127-8 epitope on MARV GP. The AGP127-8 reactivity to synthetic peptides derived from the MARV GP sequences were analyzed in ELISA. AGP127-8 exhibited strong reactivity to the peptides corresponding to amino acid positions 411–430. These amino acids are located near the GP1 cleavage site in the mucin-like region.